

# In vivo non-invasive multifrequency MR Elastography of mice liver at 7T

Tiffany Bakir Ageron, Kevin Tse Ve Koon\*, Pilar Sango-Solanas, Olivier Beuf

INSA Lyon, Université Lyon 1, CNRS, Inserm, CREATIS UMR 5220, U1294, Lyon, France  
\* Corresponding author: Kevin.Tsevekoon@creatis.insa-lyon.fr

Received date: 06/04/2024  
Accepted date: 28/06/2024  
Publication date: 31/01/2025

**Keywords:** MRE, MRI, in vivo, mice

© 2025 The Authors  
Licence CC-BY 4.0  
Published by Société de Biomécanique

## 1. Introduction

Magnetic Resonance Elastography (MRE) is a method employed to quantify tissue stiffness, as demonstrated in the context of hepatic fibrosis and providing an alternative to liver biopsy (Chen et al. 2021; Hoodeshenas et al. 2018; Yin et al. 2017). MRE usually involves three essential steps: (i) generating shear waves in biological tissue; (ii) encoding tissue displacements in the MR images and (iii) applying a dedicated reconstruction method to extract the viscoelastic parameters of tissues (Oliphant et al. 2001).

The use and development of MRE in clinical practice still presents significant challenges. Technical error rates are too high, leading to a perception of excessive uncertainty surrounding this technique (Kim et al. 2020). These issues present opportunities for improvement and preclinical studies allow for the development of innovative concepts to optimize the effectiveness and MRE performance, paving the way for potential clinical improvement and adoption in clinical routine (Bayly & Garbow 2018; Serai & Yin 2021; Sango-Solanas et al. 2022).

To date, *in vivo* MRE experiments on small animal models remain poorly documented. Given the small size of mouse organs, the use of high magnetic fields is crucial to obtain good spatial resolution with an acceptable signal-to-noise ratio (SNR). Teams working on preclinical MRE have developed invasive devices for animals, including implanting a needle into the organ of interest (Yin et al., 2017).

In this study, we propose a method to do hepatic MRE acquisitions at different excitation frequencies with a non-invasive experimental setup.

## 2. Methods

### 2.1 Experimental bench Design and MRE Setup

The experimental bench adapted for *in vivo* mouse MRE was designed with Solidworks 2016 software and includes specific features for anesthesia maintenance and shear wave generation and transmission.

Various bench components are designed to facilitate the transmission of shear waves, generated by a non-magnetic piezoelectric actuator (CEDRAT Technologies) placed away from the region of interest (ROI) to avoid susceptibility artefacts: the actuator is linked to a rigid optical fiber, transmitting mechanical excitation along the bench. A small plug is fixed to the fiber's end to aid wave propagation toward the targeted organ. MRE acquisitions were performed on a preclinical 7T MRI system (*Bruker BioSpec, Germany*) using a 40 mm inner diameter volume coil in transmit/receive mode. A waveform generator (Agilent 33220A) was configured to produce sine waves at the desired frequencies and amplitudes and amplified to feed the piezoelectric actuator.

### 2.2 Animal preparation

Experiments involving mice were performed in compliance with the European regulation on animal experimentation (Directive 2010/63/EU) and its national

transposition (Agreement NTARI2). During imaging, 3 healthy (no expected fibrosis) mice were anesthetized with 2-3% isoflurane/air via a nose cone and maintained at approximately 36.5°C using a circulating warm water heating pad. They were placed in a prone position on the above-mentioned bench. Respiratory rate and temperature were monitored throughout anesthesia.

### 2.3 MRE Sequence

The RARE (Rapid Acquisition with Relaxation Enhancement) sequence, a fast spin echo imaging method, allows rapid image acquisition by generating multiple echoes from a single RF excitation pulse. Bipolar Motion Encoding Gradients (MEG) were added on each side of the first refocusing RF pulse, ensuring a reasonable Echo Time (TE) and high SNR. The waveform generator was triggered before the start of each Repetition Time (TR) to ensure wave propagation in a stable state before encoding. Two acquisitions with opposite MEG polarities were performed for phase image subtraction and removal of static phase offsets. Four equally spaced phase offsets were acquired for complete coverage of the wave propagation period.

### 2.4 Reconstruction

Phase images acquired with positive and negative polarity were subtracted and unwrapped to obtain displacement fields, which were temporally Fourier transformed along the direction of phase offsets to isolate information at the desired frequency. Directional filtering along the wave propagation direction followed by a 4th-order spatial Butterworth bandpass filter was applied to reduce low and high frequencies noise. Finally, an Algebraic Inversion of the Differential Equation algorithm was used to extract the shear modulus  $G'$  maps (Oliphant et al. 2001) representing tissue stiffness.

## 3. Results and discussion

The *in vivo* hepatic MRE acquisitions parameters were: TR=1000ms, matrix 192x192, FOV 35x35mm<sup>2</sup>, single slice (1mm thickness). The excitation frequencies ( $f$ ) and TE are referenced in Table 1. The magnitude, displacement images and elastograms (Fig.1) were analyzed and compared. Table 1 shows the measured SNR and mean and standard deviation of  $G'$  values in the ROI placed on the liver.

**Table 1** SNR and  $G'$  measures for all mice at different frequencies

Mice	TE (ms)	$f$ (Hz)	SNR	$G'$ (kPa)
1			35.1	1.71±0.23
2	<b>14.8</b>	<b>200</b>	41.1	1.79±0.19
3			36.6	1.69±0.16
1			54.4	2.82±0.36
2	<b>8.6</b>	<b>400</b>	60.1	2.87±0.31
3			53.1	2.81±0.29
1			49.6	4.54±0.38
2	<b>10.7</b>	<b>600</b>	49.7	4.45±0.41
3			45.5	4.36±0.34

As expected, results reveal the dispersive behavior of  $G'$  with the excitation frequency:  $G'$  increases with  $f$  (Table 1). Additionally, the  $G'$  values for each frequency across the three mice are similar. The SNR varies slightly with the excitation frequency due to differences in TE values and among mice due to variability in respiratory motions.

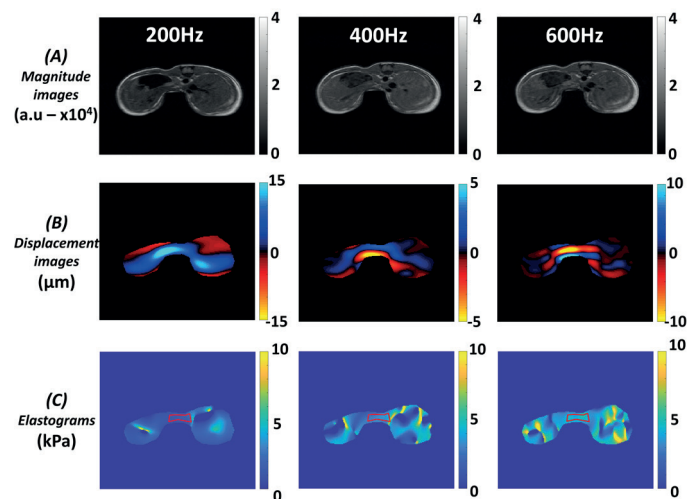


**Fig. 1** Magnitude (A), Displacement (B) images and Elastograms (C) of mouse 3

## 4. Conclusions

These promising results obtained on healthy mice confirmed the ability of the proposed method and experimental setup to assess liver stiffness at different

frequencies by observing a dispersive behavior. Next, mice with varying degrees of fibrosis will be examined alongside histological analysis. Also, efforts will focus on developing new strategies to reduce TE, improve SNR and phase encoding to explore new perspectives in MRE. Our study focused on liver stiffness in mice, future research could explore heterogeneity either due to local variations within organs or due to inter-individual differences.

## Acknowledgments

LABEX PRIMES (ANR 11 LBX 0063), PIONEER (ANR 22 CE19 0023 01), PILoT platform.

## Conflict of interest Statement

The authors declare no conflicts of interest.

## References

- Chen J, *et al.* (2021). Multiparametric MRI/MRE assesses progression and regression of steatosis, inflammation, and fibrosis in alcohol-associated liver disease. *Alcoholism: Clinical and Experimental Res.*, 45(10), 2103-2117.
- Hoodeshenas S, *et al.* (2018). MRE of Liver : Current Update. *Topics in MRI*, 27(5), 319-333.
- Yin M, *et al.* (2017). Distinguishing between Hepatic Inflammation and Fibrosis with MRE. *Radiol.*, 284(3), 694-705.
- Oliphant TE, *et al.* (2001). Complex-Valued Stiffness Reconstruction for MRE by AIDE. *MR in Med.*, 45(2), 299-310.
- Kim DW, *et al.* (2020). Comparison of technical failure of MRE for measuring liver stiffness between GRE and SE-EPI: A systematic review and meta-analysis. *JMRI*, 51(4), 1086-1102.
- Bayly PV, *et al.* (2018). Pre-clinical MRE : Principles, techniques, and applications. *JMR*, 291, 73-83.
- Serai SD, *et al.* (2021). MRE of the Abdomen: Experimental Protocols., *Preclin. MRI of the Kidney* 2216, 519-546.
- Sango-Solanas P, *et al.* (2022). Short TE dual-frequency MRE with Optimal Control RF pulses. *Scient. Rep.*, 12(1), 1406.